Phase diagram of the (Pr 1 − y Sm y) 0.7 Ca 0.3 Co O 3 system: Valence and spin state transition versus ferromagnetism

Yohann Breard, Francis Veillon, Laurence Hervé, Vincent Hardy, François Guillou, Kurt Kummer, Fabrice Wilhelm, Andrei Rogalev, Ronald Smith

Phase diagram of the $(Pr_{1-y}Sm_y)_{0.7}Ca_{0.3}CoO_3$ system: Valence and spin state transition versus ferromagnetism

Y. Bréard, F. Veillon, L. Hervé, and V. Hardy
Normandie Univ, ENSICAEN, UNICAEN, CNRS, CRISMAT, 14000 Caen, France.

F. Guillou
Inner Mongolia Key Laboratory for Physics and Chemistry of Functional Materials, Inner Mongolia Normal University, 81 Zhaowuda Road, Hohhot 010022, Inner Mongolia, People's Republic of China

K. Kummer, F. Wilhelm, and A. Rogalev
ESRF European Synchrotron, 71 Avenue des Martyrs, F-38000 Grenoble, France

R.I. Smith
Rutherford Appleton Lab, ISIS Pulsed Neutron & Muon Source, Harwell Campus, Didcot OX11 0QX, Oxon, England

The "valence and spin state transition" is a very specific transition found in some cobalt oxides, which involves a coupled modification in the Co valence and the Co^{3+} spin state. In the phase diagram of these compounds, one can thus expect a competition of this transition with the ferromagnetism associated to Co^{4+} low spin - Co^{3+} high spin double-exchange. Here we study the phase diagram of $(Pr_{1-y}Sm_y)_{0.7}Ca_3CoO_3$ and $Pr_{1-x}Ca_xCoO_3$ in order to shed some light on the competition between these two phenomena. To this end, we combine results obtained with a wide variety of techniques: magnetization, heat capacity, resistivity, neutron diffraction, x-ray absorption spectroscopy and x-ray magnetic circular dichroism. The origin of the various transition lines in the phase diagram of $(Pr_{1-y}Sm_y)_{0.7}Ca_3CoO_3$ as well as that of the "critical" value $y_{crit} \sim 0.18$ are discussed. Particular attention is paid to the nature of the groundstate magnetism which is an issue strongly debated so far in this type of cobaltates.

I. INTRODUCTION

A very peculiar type of transition is observed in some cobalt oxides, showing a concomitant change in the valence (Co^{3+}/Co^{4+}) and in the spin state (Co^{3+} low-spin / Co^{3+} high-spin) degrees of freedom. Originally discovered in well oxygenated $Pr_{0.5}Ca_{0.5}CoO_3$ [1-5] (for an overview, see for instance [6] and references therein) the field of such a « valence and spin state transition » (VSST) was progressively extended to a broader range of compositions, namely $(Pr_{1-y}RE_y)_{1-x}Ca_xCoO_3$ with RE = Sm, Eu, Gd, Tb, Y, and $0.2 \leq x \leq 0.5$ as well as $0.0 \leq y \leq 0.3$ [7-12].

In the first study on $Pr_{0.5}Ca_{0.5}CoO_3$ in 2002, Tsubouchi *et al.* [1] reported a metal-insulator transition accompanied with an abrupt drop in magnetization, a sharp peak in specific heat, and a decrease in the unit-cell volume, when cooling below the transition at $T^* \sim 90$ K. Originally, this transition was regarded as a peculiar instance of a first-order spin-state transition among the Co^{3+} (from intermediate- to low-spin state), an interpretation that remained commonly accepted for several years. Starting from 2010 however, an accumulation of data pointed to a more complex scenario. First, in a neutron powder diffraction study of $Pr_{0.5}Ca_{0.5}CoO_3$, Barón-González *et al.* [2] observed that the Co-O bonds are almost unaltered at T^*, whereas the Pr-O ones change a lot, a result leading them to suggest the possibility of a charge transfer between Co and Pr. Soon after, in their study of the heat capacity in $(Pr_{1-y}Y_y)_{0.7}Ca_{0.3}CoO_3$ compounds, Hejtmánek *et al.* [10] found a Schottky-like anomaly at $T < T^*$, a feature suggesting the presence of the Kramers ion Pr^{4+}. Then, several experiments of x-ray

absorption spectroscopy provided direct evidences of the presence of Pr^{4+} below T* in different compounds. In $Pr_{0.5}Ca_{0.5}CoO_3$ for instance, García-Muñoz *et al.* [3] and Herrero-Martín *et al.* [4] both demonstrated a partial oxidation of Pr^{3+} into Pr^{4+} when crossing *T** upon cooling.

The fact that the VSST requires the stabilization of a certain amount of Pr^{4+} at low temperatures is now widely accepted [2,3,10,13]. However, the very origin of such a mixed valence Pr^{3+} / Pr^{4+} is still a matter of debate. On the experimental side, the data on the value of this ratio is scarce and rather scattered. The only point that emerges clearly is that for a given (RE, *x*) couple, the ratio Pr^{4+} / Pr increases with *y* [10,12,14]. Experimentally, another basic issue is the competition between the VSST and the ferromagnetic (FM) ordering. In $(Pr_{1-y}RE_y)_{1-x}Ca_xCoO_3$, one expects a "critical" *y* value (y_{crit}) below which ferromagnetism (related to that of $Pr_{1-x}Ca_xCoO_3$) dominates and above which the VSST takes place. Even though one can expect a link between y_{crit} and the Pr^{4+} content in the ground state, a precise description of the crossover FM/VSST is still missing.

These various issues are addressed in the present paper. Our study was carried out in the $(Pr_{1-y}Sm_y)_{0.7}Ca_3CoO_3$ system which is well suited for an experimental investigation of the VSST. Indeed, owing to its size —slightly smaller than that of Pr^{3+}— Sm^{3+} offers the best fine control of the VSST, even though its magnetic response has to be taken into account in the analysis. A series of measurements have been conducted as a function of *y*: magnetic susceptibility, heat capacity, resistivity, as well as isothermal magnetoresistance and magnetization curves. From these data, the *y* dependencies of several characteristic temperatures have been derived: Curie temperature (T_C) , temperature of VSST (*T**), and temperature of short-range ordering (SRO) of ferromagnetic clusters (T_{SRO}). The exploration of physical properties was complemented by experiments of x-ray absorption spectroscopy (XAS) to characterize the Pr^{4+} / Pr ratio (at 5 K), and magnetic circular dichroism (XMCD) to address the spin state of Co^{3+}. On this basis, we discuss an overall description of the phase diagram, with special attention paid to the boundary between the FM and VSST regimes.

II. EXPERIMENTAL DETAILS

Polycrystalline samples of $(Pr_{1-y}Sm_y)_{0.7}Ca_{0.3}CoO_3$, with twelve compositions in the range $0 \le y \le 0.5$ were prepared by solid-state reaction, in a way similar to that previously used for $y = 0.3$ [15-18]. Starting from stoichiometric proportions of Pr_6O_{11}, Sm_2O_3, CaO and Co_3O_4 precursors, the powders were intimately ground and the mixture was pelletized in form of 2×2×10 mm bars. These bars were first sintered at 1200 °C in flowing oxygen for 30 h, and then annealed in high-pressure (130 bar) O_2 atmosphere for 80 h at 650 °C with the aim of ensuring good oxygenation of the samples.

By nature, the VSST samples entangle steric and doping effects: the former originates from the size difference between Pr^{3+} and Sm^{3+}, while the latter results from the impact of a Pr^{4+} / Pr^{3+} fraction on the Co^{4+} / Co^{3+} ratio (via charge balance). Accordingly, a second series $Pr_{1-x}Ca_xCoO_3$ ($x < 0.4$) was investigated in order to isolate the role of the doping *per se* (there is no VSST for this *x* range). Using stoichiometric mixtures of the same precursors, the bars were first sintered at 1000 °C in air for 24 h, and then annealed in flowing oxygen for 24 h at 1200 °C, before being cooled down to room temperature in 40 h. The procedure was repeated twice, after grinding and re-pelletization of the samples. Lastly, we prepared the compound $Pr_{0.7}Ca_{0.3}Ga_{0.7}Ti_{0.3}O_3$ to get a direct estimate of the Pr^{3+} magnetism in the $(Pr_{1-y}Sm_y)_{0.7}Ca_{0.3}CoO_3$ series. With Ga^{3+} and Ti^{4+} at the B sites, the only magnetic cation is Pr^{3+} at the A sites, and by keeping the same x=0.3 Ca^{2+} content on the A site the Pr^{3+} environment will be similar to that in our Co-containing compounds. The synthesis procedure was previously described in [18].

To check the purity of the samples, X-ray diffraction was performed on a X'pert Pro PANalytical diffractometer (K_α Cu = 1.549 Å), equipped with an X'Celerator detector. For a more detailed structure investigation, time-of-flight powder neutron diffraction (tofPND) data were collected at room temperature on the medium resolution, high count rate Polaris diffractometer [19] at the ISIS facility, Rutherford Appleton Laboratory, UK.

6g of each sample were loaded into an 8mm diameter thin-walled cylindrical vanadium sample canand mounted on the beamline's automated sample changer. Neutron diffraction data were collected simultaneously in all 5 Polaris detector banks for a total proton beam charge to the ISIS target of 150μAh ($y = 0$) or 400 μAh ($y \neq 0$) - where 180μAh is equivalent to ~1 hour exposure in the neutron beam. Data reduction used the Mantid software [20], with normalised diffraction patterns from banks 1,2,3 used in structure refinement (average 2θ scattering angles approx. 10°, 26°, 52° respectively).

Crystal structure refinement by Rietveld profile analysis used the Fullprof suite of programs [21]. The neutron scattering lengths used were those included in the software, and a cylindrical sample absorption correction was applied during the refinements to account for the large wavelength-dependent neutron absorption cross-section of Sm in samples with $y \neq 0$ (σa ~5900 barns at λ =1.8Å).

The magnetic data were collected using a superconducting quantum interference device magnetometer (MPMS, Quantum Design), while the heat capacity and resistivity measurements were carried out by means of a multi-purposes instrument (PPMS, Quantum Design). In addition to the temperature dependencies (2 - 400 K) of all these quantities, the field dependence of magnetization and resistivity was investigated in the ground state (T = 5 K).

X-ray absorption experiments at the Pr L_3 and Co K edges were carried out at the ID12 beamline of the European Synchrotron (ESRF) in a multi-purpose end-station [22]. The sample was mounted on a cold finger cryostat allowing the temperature of the sample to vary in the range 2.1-320 K. Partial fluorescence yield was collected in backscattering geometry using a Silicon Drift Detector mounted at 20° with respect to the incident beam.

X-ray absorption (XAS) and magnetic circular dichroism (XMCD) experiments at the Co $L_{2,3}$ edges presented in Supplemental Material [23] were carried out at the ID32 beamline of the ESRF. The experimental end-station allowed us to reach magnetic fields up to 9 T and temperature on the sample down to 5 K [24]. Bulk polycrystalline samples (~ 2 × 2 × 5 mm^3) were cleaved in an ultra-high vacuum chamber before being transferred to the superconducting magnet. XMCD spectra were recorded by flipping both the helicity of the incoming beam and the magnetic field direction.

III. RESULTS

A. Structural features

TofPND experiments in $(Pr_{1-y}Sm_y)_{0.7}Ca_{0.3}CoO_3$ have been carried out at room temperature for y = 0, 0.075, 0.15, 0.25 and 0.4. All the Rietveld refinements were successfully conducted with the P*nma* space group that is expected for distorted perovskites. The Pr, Sm and Ca atoms were found to be statistically distributed over the same crystallographic site, without any indication of ordering phenomena. In agreement with previous studies, Figure 1(a) shows that the unit-cell parameters decrease continuously when y increases, as expected from the smaller size of Sm^{3+} (1.132 Å) compared to that of Pr^{3+} (1. 179 Å) [8,25]. Due to the differences in relative atomic scattering powers between neutrons and x-rays, neutron diffraction allows us to determine much more precisely the oxygen atoms positions and therefore the Co-O-Co angles, which directly reflect the degree of distortion of

the perovskite (See details in [23]). The angle θ_1 refers to the Co-O1-Co angle involving the apical oxygen atoms, while θ_2 refers to the Co-O2-Co angle involving the basal oxygen atoms. Figure 1(b) shows that both angles decrease linearly with the increase of Sm content.

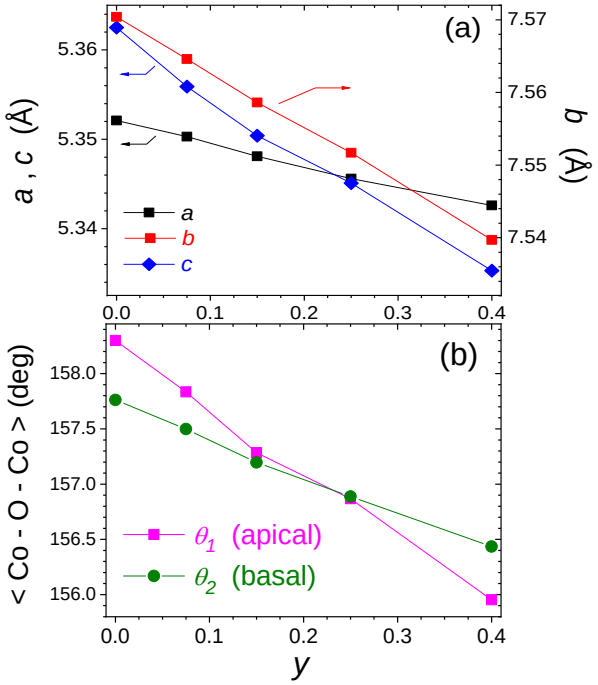

FIG. 1. Results of tofPND investigations of $(Pr_{1-y}Sm_y)_{0.7}Ca_{0.3}CoO_3$ at room temperature. (a) Unit-cell parameters as a function of y (P*nma* space group); (b) Apical and basal Co-O-Co angles as a function of y.

B. Physical properties

Figure 2 shows magnetization curves divided by the applied field (5 T) for all values of y [26]. A crossover from the FM to the VSST regime for $0.175 < y < 0.19$ is evident. In such a high field, the signature of T^* remains well defined, whereas the ferromagnetic transition is broadened (a much smaller field will be used to define the T_C, as detailed hereafter). The inset of Fig. 2 displays an enlargement of the reciprocal susceptibility around room temperature, which shows a Curie-Weiss like form. One also notes a substantial decrease of susceptibility as y is increased.

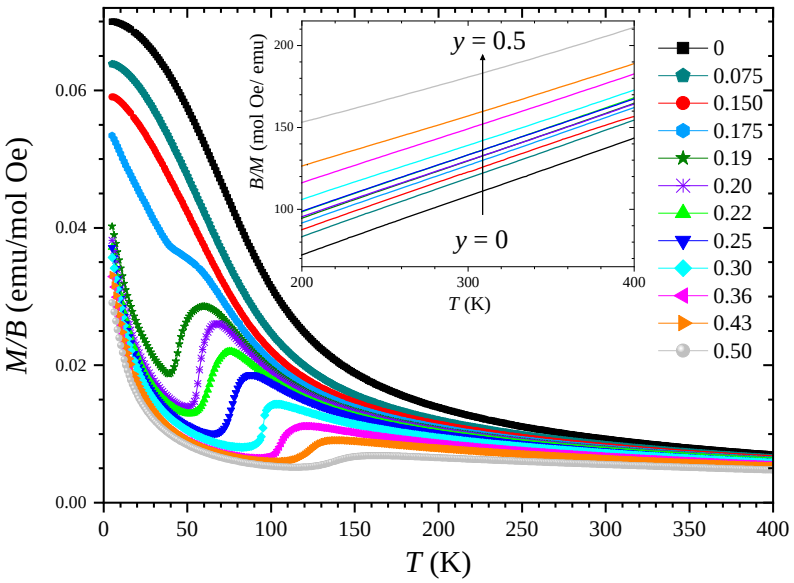

FIG. 2. Ratio of the magnetization to the applied field (5 T) as a function of the temperature, for all the investigated *y* values. The inset shows the reciprocal within the high-*T* range.

Figure 3 shows the heat capacity curves for selected values of *y*. A clear peak attributed to the VSST is visible for the largest *y* values (> 0.15). In contrast, no clear feature emerges on the *C(T)* of the compositions (≤ 0.15) situated in the ferromagnetic regime (see enlargements in [23]). It can be noted that the peak at *T** exhibits a maximum of sharpness at $y \sim 0.3$, a feature previously observed by Fujita *et al.* in this $(Pr_{1-y}Sm_y)_{0.7}Ca_{0.3}CoO_3$ system [8]. It also deserves to be noted that, for small *y* values, the low-*T* part of the curves appears as a smooth extrapolation of the high-*T* regime (following a Debye like shape), whereas the high-*y* curves exhibit a downward shift below *T**. This can be ascribed to the fact that the VSST is accompanied by a decrease in the unit cell volume upon cooling [1,7,2,27]. This induces an increase in Debye temperature when cooling below *T**, and thus a negative step in the lattice contribution (which is the greatest part of the baseline onto which the VSST peak is superimposed). The inset of Fig. 3 displays a *C/T vs.* T^2 plot of the data within the low-*T* range. For $y = 0$, one observes a straight line which indicates a response essentially made of a lattice term and an electronic one. A strong change takes place when increasing *y*, especially at the crossover FM/VSST: in addition to a decrease in the lattice term, the most prominent effect is the emergence of a Schottky peak (actually only its high-*T* wing is visible in our *T* range) that is ascribable to Sm^{3+} ($y = 0.15$), as well as to the VSST-induced Pr^{4+} (for $y > 0.15$), which are both Kramers ions.

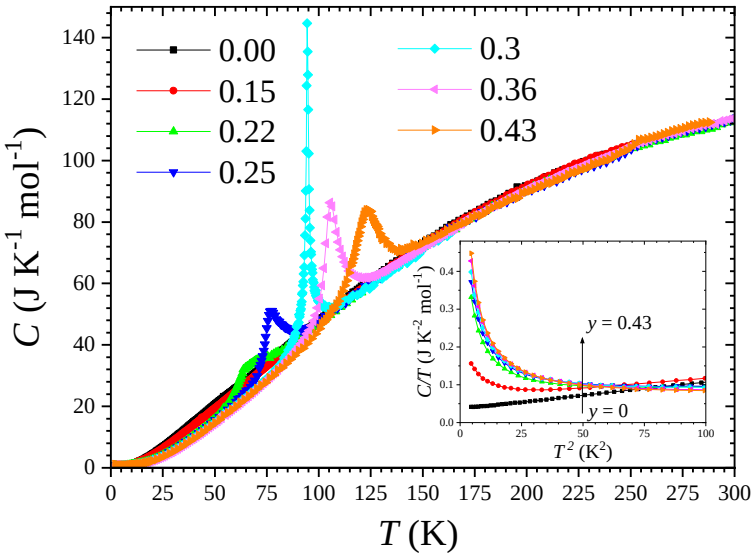

FIG. 3. Heat capacity as a function of temperature, for selected y values. The inset shows the ratio C/T vs. T^2 at $T \leq 10$ K. See [23] for details in the $C(T)$ curves for $y \leq 0.15$ and $T \leq 120$ K.

Figure 4 shows the resistivity of selected y values in a semi-logarithmic plot. The most salient feature is a sudden increase in resistivity upon cooling for the highest y values (those in the VSST regime). This transition corresponds to T^* and these compounds reach at low-T a resistivity at least four orders of magnitude higher than in low-y compounds. The latter exhibit a weak resistivity over the whole temperature range, and which can even be regarded as a metallic-like one [28]. One can also note that these curves exhibit a flat maximum within the low-T range, i.e., there is a regime of decreasing resistivity upon cooling (see inset). Such a feature can be related to a FM transition based on a double-exchange (DE) mechanism [29].

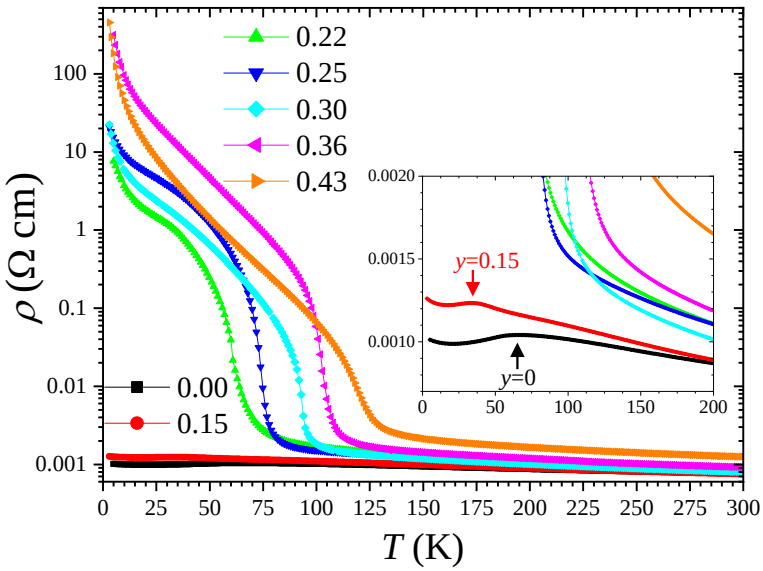

FIG. 4. Resistivity (log scale) as a function of temperature, for selected values of y. The inset is an enlargement (linear scale) for the two lowest y values, whose curve exhibit a broad hump (marked by arrows).

In Figure 5, we gather data about the field dependence of the ground state. Figure 5 (a) shows the central part of M (B: 5 T → -5 T → 5 T) recorded at 5 K for the whole y series. In the FM regime, one observes hysteresis loops with sizeable values of remanence and coercive field. The high-B part keeps a positive slope till 5 T, while its height is slightly shifted downwards as y is increased. For y > 0.175, the crossover to VSST regime is quite clear, leading to $M(B)$ curves virtually reversible (e.g. for y = 0.3, a remanent magnetization of 0.003 μ_B/f.u. and a coercive field of 80 Oe). In other respects, these curves still exhibit a marked, monotonous increase with the field. In Fig. 5(a), one of the most striking features is the absence of saturation in the FM regime, which persists up to at least 14 T (see [23]). This behavior is in line with previous studies and it can be at least partly ascribed to the rare-earths magnetism.

Figure 5(b) shows the field dependence of the magnetoresistance, ($MR = [\rho(B) - \rho(0)]/\rho(0)$) recorded at 5 K within the y series (measuring path +9 T → -9 T). The crossover FM/VSST has a very visible impact, inducing changes in both the shape and sign of the $MR(B)$ curves. The negative MR of the samples in the VSST regime is consistent with previous reports in related systems [30]; in contrast, the positive MR found at the FM side is much more unusual. Curiously, we were unable to find in the literature previous results on the MR at low-T for y = 0 ($Pr_{0.7}Ca_{0.3}CoO_3$), despite the many studies carried out on this compound. For the y values of Fig. 5(b), $\rho(B)$ curves were recorded at regularly spaced temperature up to 140 K. The curves $MR(T)$ extracted from these data exhibit peaks located either at T_C or at T^*, depending on the y value (see [23])

From Figs 5(a) and (b), we derived the y dependencies of the remanent magnetization [Fig. 5(c)] and of the magnetoresistance [Fig. 5(d)] at 5 K. In both cases, a sharp crossover takes place at a critical value y_{crit} ~ 0.18, separating the FM and VSST regimes.

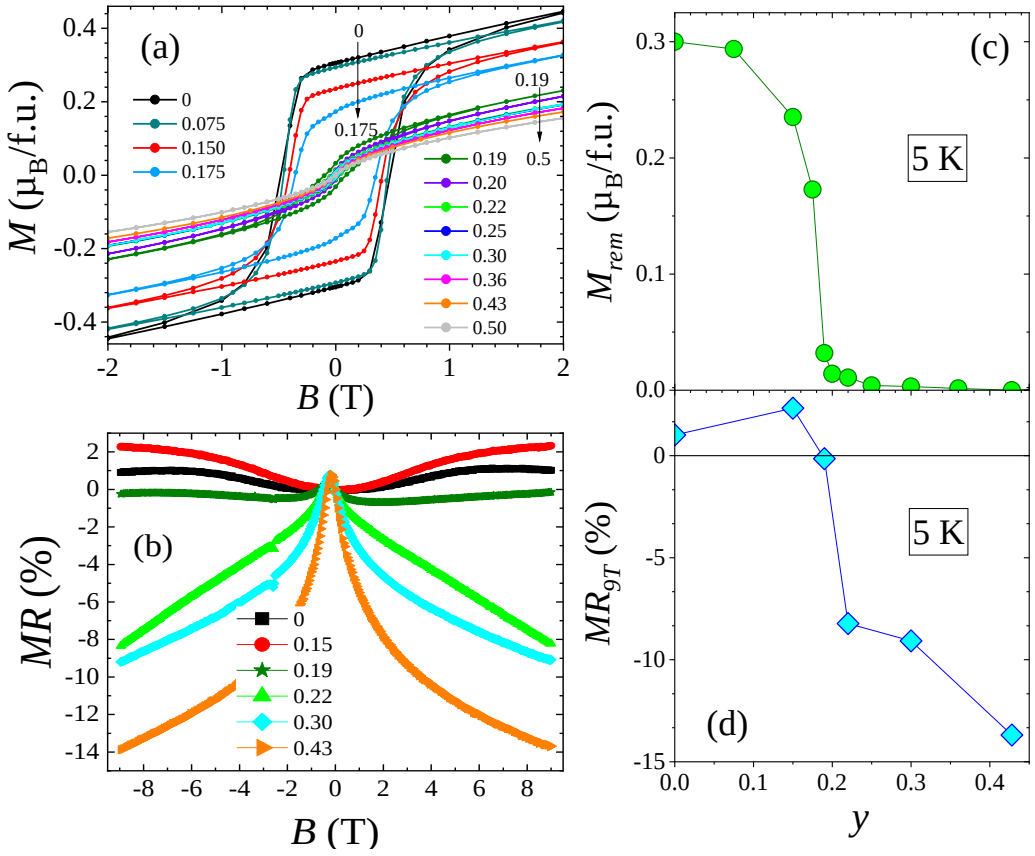

FIG. 5. (a) Magnetic hysteresis loops at 5 K for all the *y* values. (b) Magnetoresistance [*MR*=100 {$\rho(B)$- $\rho(0)$}/$\rho(0)$] at 5 K for selected values of *y*. (c) Remanent magnetization derived from (a) as a function of *y*. (d) Magnetoresistance at 9 T derived from (b), and plotted as a function of *y*.

C. Phase Diagram

The characteristic temperatures of the $(Pr_{1-y}Sm_y)_{0.7}Ca_3CoO_3$ system were primarily derived from magnetic measurements, which led us to address the impact of the following three issues: value of the measuring field, hysteresis, and training effect (see [23]). The latter stems from the first-order nature of the VSST, which requires the sample to accommodate the structural distortion at the transition. In such a case, several crossings of the transition can be necessary before finding a reproducible "transition path". In our compounds, this effect was found to be limited to the first cooling, which was thus systematically discarded from our analysis. The hysteresis across the VSST is still an active subject of debate. It is now admitted that it is not as high as initially reported, and that it is actually very dependent on the sweep rate [31]. It remains that a small hysteresis seems to persist even for quasi-static measurements, especially in case of the lowest *T**, i.e., for the lowest *y* values [31,32]. To avoid related scattering, we considered the field cooled warming (FCW) mode at a rate of 0.5 K/min. The value of the measuring field impacts only weakly the *T**, whereas it is mandatory to use a low field to get a reliable value of T_C. For this purpose, we used either 10 Oe in FCW mode, or preferably, the inspection of the spontaneous magnetization (M_{spont}), i.e., when cooling in the residual field of the superconducting coil after demagnetization (~ 1.5 Oe).

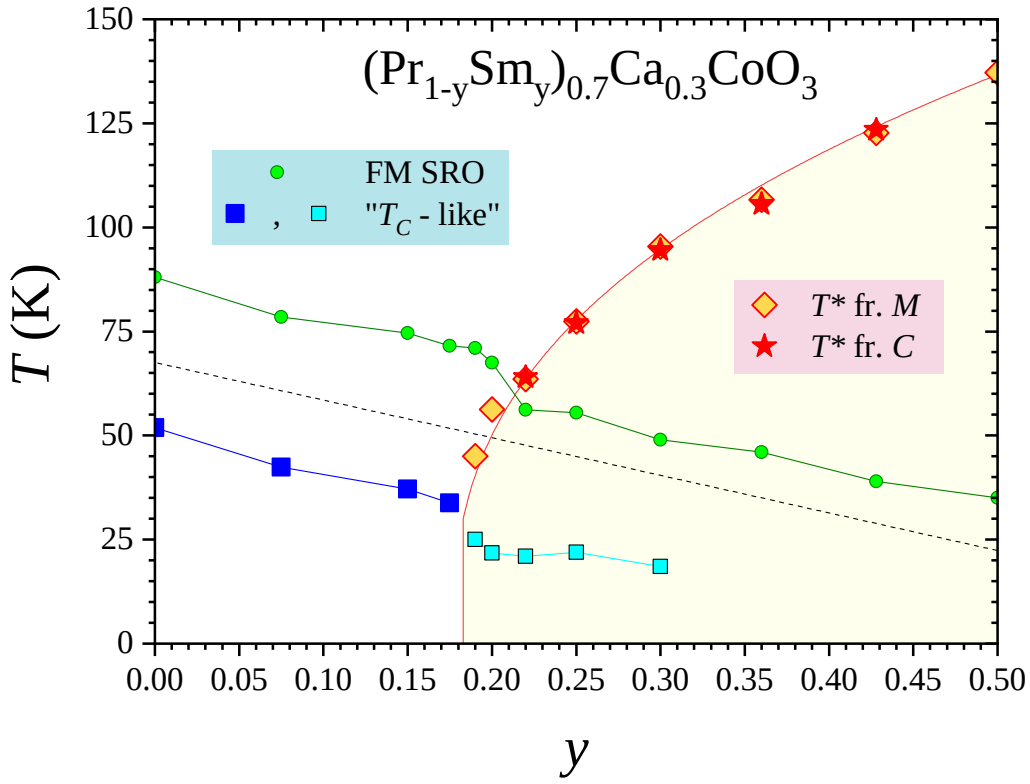

FIG. 6. Phase diagram of the system $(Pr_{1-y}Sm_y)_{0.7}Ca_{0.3}CoO_3$. See [23] for illustrations of the criteria used to determine the characteristic temperatures. The *T** line is derived both from the position of the inflection point on the *M(T)* curves and that of the peak on the *C(T)* ones. The thin red line is a fitting function of the form $(y\text{-}y_{crit})^n$ (see text). The FM SRO line is derived from the kink on dM_{spont}/dT (where M_{spont} is the spontaneous magnetization measured upon cooling in a field of ~1.5 Oe). The

squares are ascribed to the predominant Curie temperature of the distribution of FM clusters. These characteristic temperatures are derived from the presence of a minimum in $[dM_{spont}/dT](T)$. On the low-y side, it simply reflects the midpoint of the ferromagnetic ordering [absolute minimum in dM_{spont}/dT], whereas it rather corresponds to a local minimum for larger y values. The dashed line shows the expected dT_C/dy calculated from data of the literature on cobaltates (see Section IV.A.2).

In our phase diagram, the characteristic temperatures are based on the derivative of M_{spont} (see [23]). A negative maximum of dM_{spont}/dT was ascribed to T_C; this definition is akin to the usual "midpoint" criterion applied to the rise of magnetization upon cooling. Since this feature is considerably weaker above y_{crit} than below it, the $T_C(y)$ line will be divided into two parts. A positive maximum of dM_{spont}/dT is ascribed to T^*; this reflects the positive step in (paramagnetic) magnetism that is associated with a change from (Pr^{4+},Co^{3+}LS) to (Pr^{3+}, Co^{4+} LS,Co^{3+}HS) when crossing T^* upon warming [16]. Finally, the T_{SRO} is connected to the takeoff of dM_{spont}/dT upon cooling; we found it also corresponds to the start of a non-linear magnetic response.

The phase diagram resulting from these $T_C(y)$, $T^*(y)$ and $T_{SRO}(y)$ lines is shown on Fig. 6. We added to this plot the position of the maxima in $C(T)$, which can be regarded as another signature of T^*. The inflection points on the resistivity curves are also found to be well consistent with these lines (see [23])

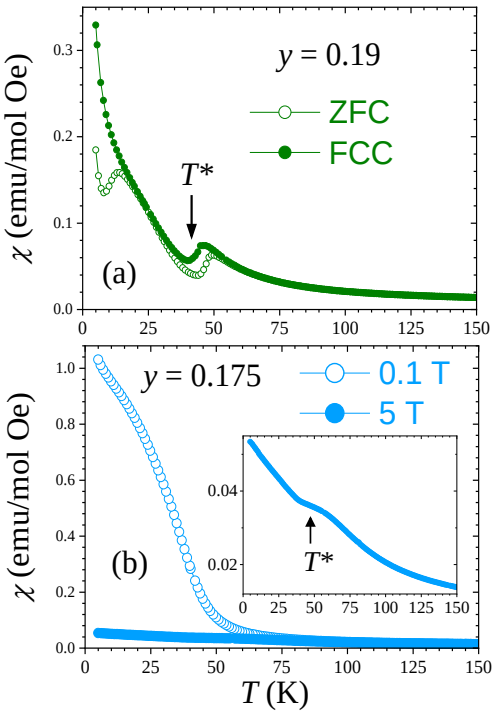

FIG. 7. Curves of *dc* susceptibility (M/B) versus temperature: (a) Zero-field-cooled and field-cooled-cooling curves recorded in 0.1 T for y = 0.19; (b) Field-cooled-cooling curves recorded in 0.1 and 5 T for y = 0.175. The inset is an enlargement of the high-B curve revealing a signature of T^*.

D. Boundary FM/VSST

The $T^*(y)$ data is fitted to a function of the form $(y\text{-}y_{crit})^n$, leading to y_{crit} =0.177 and n = 0.38. Hereafter, we will keep the rounded value y_{crit} ~ 0.18. Let us emphasize that this y_{crit} marks a *change in the hierarchy* between the FM and VSST regimes, but the two transitions can coexist. This is evident on Fig. 7(a) in the case of y = 0.19 (> y_{crit}), where one can observe below T^* the signature of T_C, that is here clearly highlighted by the bifurcation between the ZFC and FCC branches. Very similar features were observed for y = 0.0625 in the (Pr_{1-}

$_yY_y)_{0.7}Ca_3CoO_3$ system [32]. On the other side, Fig. 7(b) shows that a signature of T^* can be observed for y = 0.175 ($< y_{crit}$) , when applying a magnetic field large enough to spread out the FM transition.

In mixed valent cobaltates, the FM response is intimately related to the Co^{3+}/Co^{4+} ratio. Since the y_{crit} value involves the strength of the FM response, it must be indirectly connected to the Pr^{4+}/Pr^{3+} ratio. A basic question is thus to tackle the intrinsic y dependence of this Pr^{4+} content at low-T. To do so, XAS experiments is undoubtly the most suited tool.

E. Pr valence at low T

Let us first summarize the literature on this issue. In the archetypical VSST compound $Pr_{0.5}Ca_{0.5}CoO_3$, a large range of values are reported (Pr^{4+}/Pr values at low-T are between 0.15 [4] and 0.26 in [3]). In $(Pr_{1-y}RE_y)_{1-x}Ca_xCoO_3$ systems, the Pr^{4+}/Pr ratio was shown to increase with y; this was studied in detail in the case x = 0.3 for both Y and Tb: For RE = Y, when y is doubled from 0.075 to 0.15, Pr^{4+}/Pr goes from 0.15 to 0.27 [14]; For RE = Tb, when y is doubled from from 0.1 to 0.2, Pr^{4+}/Pr goes from 0.19 to 0.25 [12].

The present work addresses the case RE = Sm, with nine y values between 0 and 0.43. The Pr valence was determined from Pr L_3 spectra using a method similar to that previously employed for VSST materials [3,4,6,14,18]. The Pr L_3 edge was fitted by a combination of 1 arctangent (accounting for the edge jump), 1 lorentzian forming the main white line representative of Pr^{3+}, and 2 lorentzian functions representative of Pr^{4+} (about 5 eV and 12 eV above the main white line), see spectral decomposition in Ref. [18]. The Pr^{4+} fraction is then calculated from the ratio of the integrated intensity of the lorentzian functions. The results of Pr^{4+}/Pr vs. y at T = 5 K are shown in Fig. 8. As y is increased, the increase in Pr^{4+}/Pr exhibits a S-like shape with an inflection point around y = 0.18, i.e., a value close to y_{crit}.

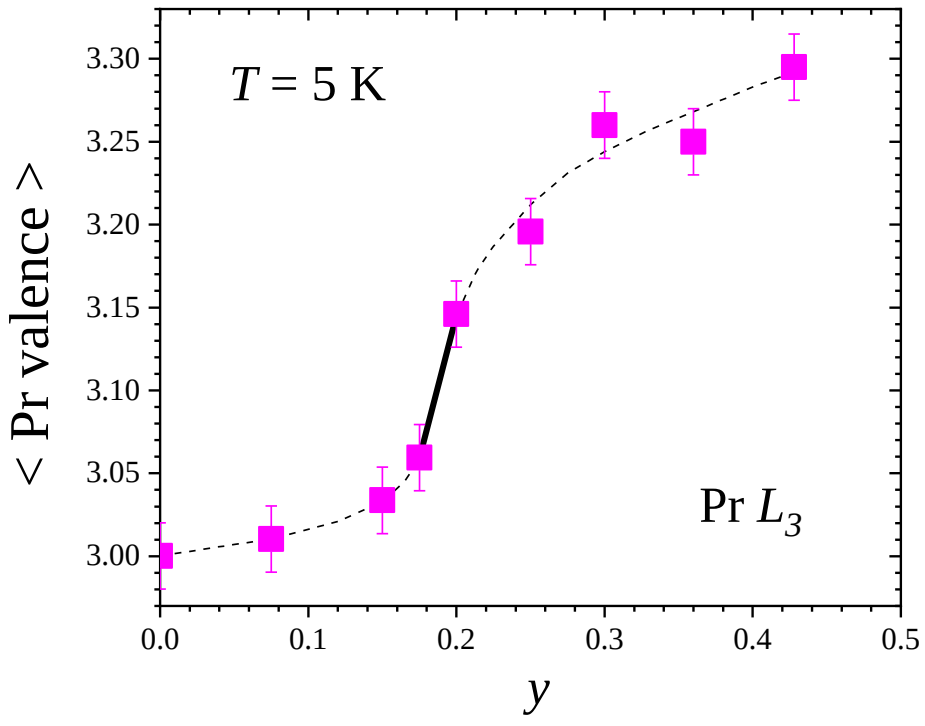

FIG. 8. Average Pr valence at 5 K, derived from the analysis of XAS measurements at the Pr L_3 edge. The dashed line is a guide to the eye. Note the presence of a weak but undeniable jump between y ~ 0.175 and y ~ 0.20 (thick solid line).

F. Doping effect

The interest in the series $Pr_{1-x}Ca_xCoO_3$ is to deconvolute the doping effect from the others in the analysis of the VSST transition. In this series, the doping corresponds to the ratio Co^{4+}/Co that is directly given by x. For sufficient level of doping, FM related to a double-exchange mechanism between Co^{4+} and Co^{3+} takes place. In other respects, the Co^{3+} can undergo a spin-state transition (SST) from LS to HS as the temperature is increased.

Susceptibility curves were recorded for eight values of x in the range 0-0.4 (raw data in [23]). To remove the Pr contribution, we employed a direct subtraction method [33,34] using the susceptibility of Pr^{3+} proposed by Tsubouchi *et al.* [35]: $\chi^{Pr^{3+}}(T) = 1.6/(T+54)$ emu/mol. Figure 9(a) displays the resulting curves reflecting the cobalt susceptibility χ^{Co}, for selected values of x. The T_{SST} and T_C temperatures were derived from a rise in $\chi^{Co}(T)$ and a negative maximum in $d\chi^{Co}/dT$ as T is increased, respectively (see details in [23]). The x dependencies of these characteristic temperatures is reported in the phase diagram of Fig. 9(c). These lines are well consistent with those previously reported by El-Khatib *et al.* [36], except that we did not find evidence of a short-range ordering line around 250 K (see [23]).

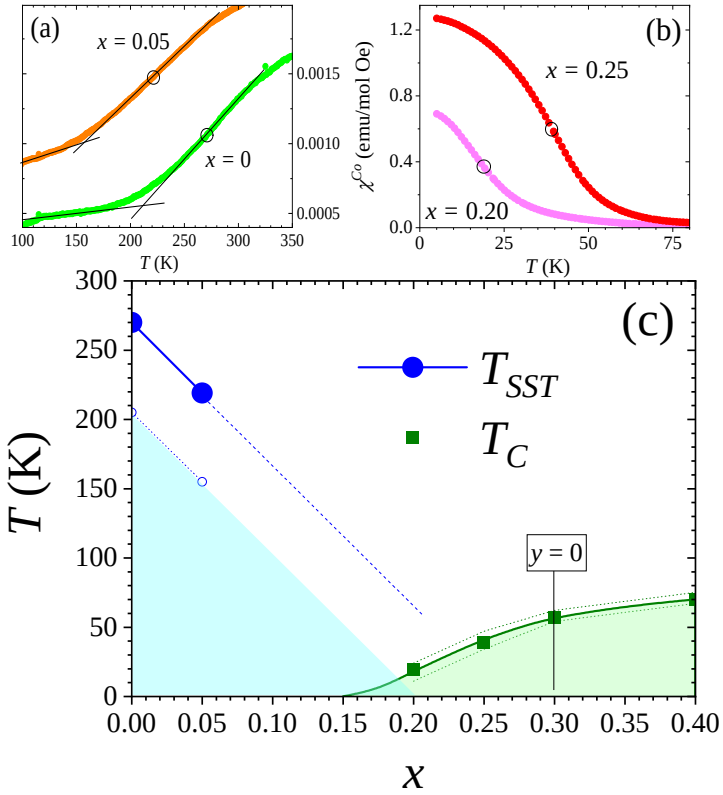

FIG. 9. Magnetic investigation of the $Pr_{1-x}Ca_xCoO_3$ series. Panels (a,b) shows susceptibility curves recorded in 0.1 T for selected x values. The contribution from the Pr^{3+} ions has been removed to isolate the Co response (see text). Panel (a) refers to the low-x range, in which the rise in $\chi^{Co}(T)$ is associated with the spin-state transition (SST) of Co^{3+} from LS to HS. The characteristic T_{SST} is associated with the midpoint of the transition (circles) while the beginning of the SST is derived from the crossing point between two linear extrapolations of $\chi^{Co}(T)$. Robust signature of these features is no longer discernable for $x > 0.05$. Panel (b) corresponds to the high-x regime where a clear FM response takes place. The T_C is derived from the point of maximum slope in $\chi^{Co}(T)$ (circles). Panel (c) displays these temperatures as a function of x, which represents the fraction of tetravalent cobalt. Also shown are the beginning of the SST (open circles) and maxima in $\partial^2(\chi^{Co})/\partial T^2$ on the FM side (dotted green lines)

which reflect the width of the Curie transition. The blue dashed line is an extrapolation of the $T_{SST}(y)$ line, aimed to materialize the interplay with the FM regime.

IV. DISCUSSION

A. Phase Diagram

Apart from the SRO lines, the most salient features of the phase diagram of Fig. 6 are: (i) existence of a y_{crit} separating two regimes, dominated either by FM or VSST; (ii) below y_{crit}, the T_C decreases as y increases; (iii) above y_{crit}, the T^* increases as y increases. These features are in line with previous results of the literature on VSST. In $(Pr_{1-y}Sm_y)_{0.7}Ca_3CoO_3$, Fujita *et al.* [8] showed that the spin-state transition (SST, the "valence" character of the transition being unknown at that time) takes place at a temperature that increases as y is increased, from $y \sim 0.2$ till ~ 0.8; the lower boundary was ill defined, but there was no SST for $y = 0.1$. Soon after, Wang *et al*. explored the same system with increased resolution in y, and they found a FM/SST boundary at $y_{crit} \sim 0.175$ [37]. Investigation of the closely related $(Pr_{1-y}Eu_y)_{0.7}Ca_3CoO_3$ showed the same qualitative behavior, with $y_{crit} \sim 0.19$ [11]. Actually, the most studied system in VSST literature is $(Pr_{1-y}Y_y)_{0.7}Ca_3CoO_3$, owing to the fact that Y^{3+} is non-magnetic, which facilitates the analysis [10,14,27,30,32,38-40]. However, the size difference with Pr^{3+} is quite strong, [41] which makes it difficult to follow the emergence of the VSST. In this system, Hejtmanek *et al.* [6] found that the lowest y value of their series ($y = 0.0625$) is enough to switch the system into the VSST regime. In a later study, [30] it was shown that y_{crit} is still lower, i.e. < 0.05. In practice, no compound characteristic of the FM regime was reported in $(Pr_{1-y}Y_y)_{0.7}Ca_3CoO_3$ for $y \neq 0$. The present study on the $(Pr_{1-y}Sm_y)_{0.7}Ca_3CoO_3$ system has the advantage to provide us with a quite complete phase diagram, encompassing the FM and VSST regimes, and allowing a fine inspection of the crossover between them.

1. *Crossover FM/VSST: y_{crit}*

Phelan *et al.* emphasized that the emergence of a Pr^{4+} fraction in VSST compounds can shift the Co^{4+}/Co^{3+} ratio below the threshold for ferromagnetism [30]. To investigate this issue in detail, let us consider the phase diagram established for $Pr_{1-x}Ca_xCoO_3$ [Fig. 9(c)] and the Pr^{4+} (y) plot of Fig. 8. The Pr^{4+} content exhibits a jump around $y_{crit} = 0.18$. The low y side of this jump corresponds to $y = 0.175$ (with an average Pr valence of 3.06), a composition for which the main transition is a T_C (see Fig. 6). It corresponds to an amount of Pr^{4+} per f.u. — noted $[Pr^{4+}]$— given by $0.06\times0.7\times(1-0.175) = 0.035$, and thus an amount of Co^{4+} per f.u. equal to $(0.3-0.035) = 0.265$. In Fig. 9, one can see that for such a doping level (keeping in mind that x corresponds to the ratio Co^{4+}/Co), the FM regime is clearly dominant, with $T_C > T_{SST}$ (if any). In Fig. 8, the high-y side of the jump in Pr^{4+} (y) corresponds to $y = 0.20$ (Pr valence 3.15), for which the main transition has now turned into a VSST (see Fig. 6). This y value corresponds to $[Pr^{4+}] = 0.084$ and thus $[Co^{4+}] = 0.216$. It turns out that this latter value lies in a range of doping where one can speculate that the hierarchy between FM and VSST has been reversed, i.e. $T_{SST} > T_C$, [Fig 9(c)]. In the end, it thus appears that the jump in Pr^{4+} (y) is remarkably consistent with the phase diagram of $(Pr_{1-y}Sm_y)_{0.7}Ca_3CoO_3$ when taking into account the influence of the doping level (Co^{4+}/Co) on the hierarchy between SST and FM ordering.

2. *T_C versus y*

First of all, one must address the nature of the ferromagnetism in the low y range. This issue is still intensively debated in the prototypical case of $y = 0$. In 2004, it was claimed that $Pr_{0.7}Ca_{0.3}CoO_3$ is not a genuine ferromagnet [42] and that its magnetism is inhomogeneous [43]. The possibilities of a phase separated state [42] or of a spin glass [44] were proposed, but the question has remained unsolved. More recently, new experimental data reactivated the controversy, in particular spectra of small angle neutron scattering [36] and the analysis of Schottky terms in heat capacity measurements [28]. The former were found to support a model of phase separation (PS), whereas the latter led to claim an homogeneous magnetism. Overall, our data rather lends support to a PS picture, one of the most significant arguments being the absence of a clear peak in $C(T)$, while there is a sharp rise in $\chi(T)$ upon cooling. We consider this is not compatible with a bulk ferromagnetism involving 100% of the volume. It remains that there is a very clear FM-like response, and that the domains in which it develops can be quite large [30].

About the dependence $T_C(y)$, it is known that a decrease in $<r_A>$ reduces the Co-O-Co angle, which in turn opposes the setting of a FM state (via double-exchange) [28,45,46]. This effect is present when increasing the content of Sm^{3+} that has a smaller ionic radius than Pr^{3+}. As y is increased, it is thus expected to observe a decrease in the temperature of FM ordering, both for the T_C and T_{SRO} lines (which actually exhibits the same slope versus y in Fig. 6). To be more quantitative, let us consider the literature on cobaltates. Considering $RE_{0.7}AE_{0.3}CoO_3$, we collected data of T_C versus $<r_A>$ for various rare-earths and alkaline-earths [28,47]. This data is found to obey a linear law within the relevant range of cationic radius : $dT_C / d<r_A> =$ 2734 K/Å (see [23]). In the $(Pr_{1-y}Sm_y)_{0.7}Ca_3CoO_3$ series, the dependence of $<r_A>$ versus y is linear too : $d <r_A> /d y = 0.7[r_A(Sm^{3+})-r_A(Pr^{3+})] = -0.0329$ Å. Therefore, we anticipate a slope $dT_C / dy = (dT_C / d<r_A>)(d<r_A> /dy) = -$ 90 K, that is plotted on Fig. 6. It turns out that the experimental dT_C / dy is in good agreement with this value. This supports the idea that the FM signatures in this system (including SRO) are related to the double-exchange mechanism.

3. T versus y*

In the VSST regime above y_{crit}, one observes that T^* increases as a function of y. One expects the position of T^* to be linked to the gap of the SST (Co^{3+} LS towards Co^{3+} HS) which depends not only on the crystalline electric field (CEF), but also on the cobalt bandwidth (W), as evidenced by isotopic effect (^{16}O / ^{18}O) in $y = 0.3$ [37]. Actually, it was suggested that one should consider as the SST gap, the quantity $\Delta_{SST} = (\Delta_{CEF} - \Delta_{Hund}) - (W/2)$, where Δ_{Hund} is the Hund coupling energy, while W is proportional to the Co-Co transfer energy which itself varies as the angle Co-O-Co [48].

Increasing y in $(Pr_{1-y}Sm_y)_{0.7}Ca_3CoO_3$ induces a decrease in $<r_A>$, which in turn decreases the distance Co-O and the angle Co-O-Co. As a consequence, Δ_{SST} is expected to increase owing to both a larger Δ_{CEF} (via decreasing Co-O) and a smaller W (via decreasing Co-O-Co). This dual effect can explain the increase of T^* as y is increased. Quantitatively, it must be emphasized that the angle effect strongly dominates over the distance one [7-8]. One can also note that the impact of an increase in Co-O-Co on T_{SST} is not linear [49], which is in good accordance with the observed rounded shape of $T^*(y)$ in Fig. 6.

4. Curie-Weiss regime at high temperature

Another aspect of the evolution of magnetism along the $(Pr_{1-y}Sm_y)_{0.7}Ca_3CoO_3$ series is the decrease of susceptibility at high temperature as y increases (see inset of Fig. 2). To isolate the Co response, one must first remove the contributions from Pr and Sm. For the former, we used the susceptibility measured on $Pr_{0.7}Ca_{0.3}Ga_{0.7}Ti_{0.3}O_3$ [representative of $\chi(Pr^{3+})$ in

conditions very close to ours), and for the latter the expression derived from $SmCoO_3$ by Ivanova *et al.* [$\chi(Sm^{3+}) = (1.4\ 10^{-3} + 0.0276/T)$ emu/mol] [50]. Then, one needs to consider the diamagnetic component χ_{dia} = -0.63 10^{-4} emu/mol, as well as a temperature-independent term, referred to as χ_0. This χ_0 incorporates several contributions among which the most important are Pauli and van Vleck terms [51].To complement the magnetic data, XAS experiments were carried out to investigate the Co^{3+} spin state at room temperature (see [23]) . It was found that the nature of the HS/LS mixture is only slightly affected by the *y* value in this *T* range. The fitting of the XAS spectra yields a percentage Co^{3+}HS/Co at room temperature of approximately 42%, 37% and 34% for *y* = 0, 0.3 and 0.36, respectively.To get μ_{eff} consistent with these XAS results, we were needed to set χ_0 = 5 10^{-4} emu/mol, which lies within the range of expected values (see [23]). In the end, our estimate of the cobalt susceptibility χ^{Co} at high temperature is obtained by calculating:

$$\chi^{Co}(y,T) = \chi(y,T) - 0.7(1-y)\chi(Pr^{3+},T) - 0.7y\,\chi(Sm^{3+},T) - \chi_{dia} - \chi_0. \quad (1)$$

The reciprocal susceptibility curves [Fig. 10(a)] show the persistence of an upward shift as *y* is increased, demonstrating that this feature is intrinsic to the Co response and does not only comes from the difference in magnetism between Pr^{3+} and Sm^{3+}. On closer inspection, one also observes that the $1/\chi^{Co}(T)$ curves tend to exhibit a concave upward shape for the highest *y* values. However, these curves correspond to the lowest χ values, so they are expected to be the most affected by the experimental uncertainties; since the XAS experiments at room temperature have shown that the ratio Co^{3+} HS/Co is weakly affected by *y*, we made a CW analysis of the curves in Fig. 10(a) by assuming the same slope for all of them (so just reducing the fitting range for highest *y* values). Figure 10(b) displays the θ_{CW} derived in such a way, from the linear intercepts to the temperature axis. As *y* is increased, one observes a continuous decrease in θ_{CW} with a striking change in sign from positive to negative.

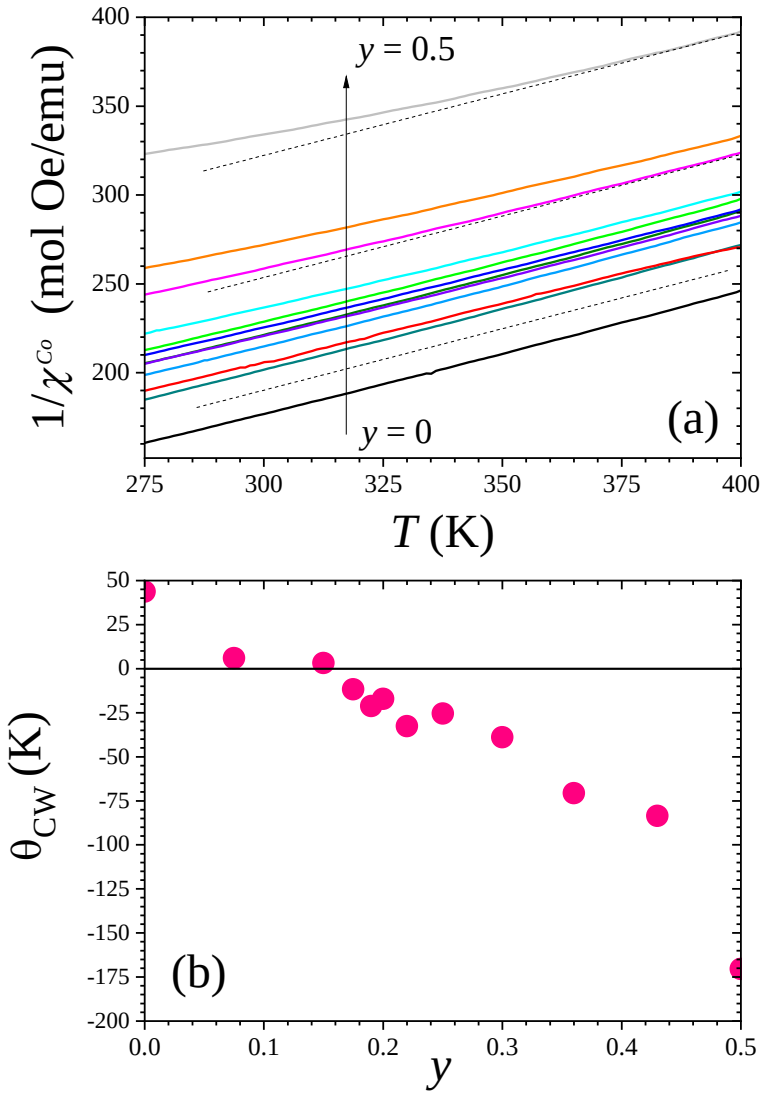

FIG. 10. Reciprocal Co susceptibility at high temperatures, for all the *y* values. The dashed lines have the slope derived from the curve of $y = 0$. (b) Curie-Weiss (CW) temperatures as a function of *y*, when using the χ^{Co} susceptibility of (a) and assuming a Co^{3+} spin state independent of the Sm content at room temperature.

Within the $(Pr_{1-y}Sm_y)_{0.7}Ca_3CoO_3$ system, the magnetic interactions bring into play a competition between a double-exchange (DE) mechanism involving Co^{4+} LS-Co^{3+} HS, and super-exchange (SE) couplings dominated by the one associated to Co^{3+} HS-Co^{3+} HS. For a matter of Co-O-Co angle, the ferromagnetic DE mechanism is progressively weakened as *y* is increased, which thus enhances the signature of the SE interaction Co^{3+} HS-Co^{3+} HS, which is antiferromagnetic. This phenomenon can explain the observed crossover between positive and negative θ_{CW} values as a function of *y*. We note that a similar behavior was previously reported in $La_{1-x}Ca_xCoO_3$ [52]. Let us also add that the θ_{CW} for the largest $y = 0.5$ (-175 K) becomes close to that of $LaCoO_3$, whose estimates span a range from -160 K to -250 K [51-55]. This can be ascribed to the fact that DE is virtually quenched for such a large $y = 0.5$, while the SE Co^{3+} HS-Co^{3+} HS in our compounds corresponds to a ratio Co^{3+} HS/Co close to 40%, which is very similar to the situation in $LaCoO_3$.

5. Nature of the SRO features

In the present study, short-range ordering (SRO) features have been identified both in the FM and VSST regimes. Note that we prefer to keep the denomination SRO even though it was reported that some of the clusters can spread over rather large length scales, reaching several tens of Å [36]. The basic question to be addressed is the nature of these clusters and of the associated ferromagnetism.

To do so, let us consider the case of $y = 0$ ($Pr_{0.7}Ca_{0.3}CoO_3$). From XMCD of Co at 5 K (see [23]), we isolated the magnetic response of Co which yields a $\mu^{Co}(B)$ very well consistent with that derived when subtracting the Pr signal from a $M(B)$ curve [27]. The shape at low-B is the one displayed in Fig. 5(a) ; increasing the field above 2 T confirms the absence of saturation up to 9 T (XMCD) and even up 14 T (magnetization). While the remanent magnetization of $0.3\mu_B$ per Co could well correspond to the response of Co^{4+} LS ($S = 1/2$) [27,28], the larger values of magnetization observed in high field are problematic. Basically, this is incompatible with a scheme where all the Co^{3+} are LS, so one has to consider that a fraction of them is in a higher spin state. About the alternative between intermediate or high spin states for Co^{3+}, our previous studies lead us to favor the second possibility, with a mixture LS/HS [15,18]. Following similar reasoning, Knížek *et al.* suggested the existence of a small fraction of Co^{3+} HS related to oxygen defects [27]. Considering that $Pr_{0.7}Ca_{0.3}CoO_3$ is on the borderline of a SST (LS/HS), such a small fraction of Co^{3+} HS at $T << T_{SST}$ could also simply be regarded as a mark of the low-T tail of the transition. The clusters would correspond to the zones around these Co^{3+} HS, into which the coexistence with Co^{4+} LS neighbors can trigger FM interaction via DE. Accordingly, the SRO would mark the ferromagnetic ordering of these clusters, leading to a phase separated state since these clusters are embedded into a non-FM matrix where the Co^{3+} are LS.

In $Pr_{0.7}Ca_{0.3}CoO_3$, the increase in susceptibility as T is decreased is very broad, indicating an inhomogeneous magnetic ordering of the clusters. The most likely reason is the statistical variety of local configurations involving (Co^{4+} LS / Co^{3+} HS / Co^{3+} LS) which can induce a broad distribution of SRO temperatures. In such a vision, the temperature we referred to as the "T_C" should be regarded as the value of Curie temperature associated with the most probable local configuration of cobalt cations.

Turning back to the $\mu^{Co}(B)$ curve at low-T, we claim it can be described by the combination of two mechanisms: alignment of FM domains and polarization of the background. The former is associated to the clusters involving the couple (Co^{3+}HS / Co^{4+}LS) and it is responsible for the "hard" FM features, i.e. remanence and coercivity; the latter is associated with the surrounding matrix involving (Co^{3+}LS / Co^{4+}LS), and it is responsible for the "smooth" increase of magnetization as the field is increased. Using rough spin-only estimates of the magnetic moments for Co^{3+} HS (4 μ_B) and Co^{4+} LS (1 μ_B), the assumption of a fraction Co^{3+} HS/Co^{3+} equal to about 10% would lead to a saturation magnetization of $(0.7\times0.1\times4) + (0.3\times1) = 0.58$ μ_B, compatible with XMCD and magnetization data.

The above description of FM clusters is also relevant to the VSST side of the phase diagram, both for the T_{SRO} and the T_C-like lines. For each of them, one observes that their portions on the two sides of y_{crit} are located in the continuation of one another, but there is a downward shift when entering the VSST regime. This originates from the fact that the VSST induces a decrease in the doping level (Co^{4+}/Co), which yields in turn a decrease in the temperature of FM ordering [see Fig. 9(c)].

The magnetoresistance can be useful to shed light on the nature of SRO [30]. Let us focus here on the ground state that was investigated by *MR* measurements at 5 K. On the VSST side (large y values), the large negative *MR* is consistent with what is expected in phase-separated systems involving metallic-like FM clusters. Quantitatively, one can even note that -15% in 9 T for $y = 0.43$ is close to what is observed in $(Pr_{0.9}Y_{0.1})_{0.7}Ca_{0.3}CoO_3$ for

similar values of T^* [30]. Supporting the similarity with Ref. [30], we also observed an hysteresis in the *MR(B)* curves (~ ± 0.2 T around zero-field) which is consistent with a vision of intercluster negative *MR*. In contrast, the *MR* in the FM regime (being both lower in absolute value and positive) is much more puzzling.

Actually, positive *MR* is quite rare in transition metal oxides. In a study on $La_{1-x}Ca_xCoO_3$ for $x \sim 0.25$, similar results were reported, but no clear conclusion could be reached about the origin of this positive *MR* [56]. Various possible origins for such positive MR at low-*T* in oxides are reviewed in [56], but none of them can be unambiguously applied to our data. Moreover, in the present case of $(Pr_{1-y}Sm_y)_{0.7}Ca_3CoO_3$ compounds, Fig. 5(b) shows a change in curvature of *MR(B)* as the field is increased, pointing to a competition between (at least) two mechanisms of opposite signs [57]. One can be reasonably confident about the nature of only one of them, i.e. the negative *MR* present in the VSST samples (large *y* values) which can likely be ascribed to a mechanism of tunneling between FM clusters within a non-FM matrix. As for the positive *MR*, we suggest it might result from the very peculiar type of phase separation in low *y* compositions, where the density (and maybe also the size) of FM clusters is much higher than for high *y*.

B. Structural origin of the Pr mixed valence

A central issue for the understanding of the VSST is the origin of the stabilization of a Pr^{4+} fraction at low *T*. First, it can be recalled that Pr is prone to exhibit mixed valence (3+/4+) including in oxides, e.g. in Pr_6O_{11}. If focusing attention to the case of perovskite, the best known example is that of $BaPrO_3$, where Pr sits on the B sites. Mixed valence was also found with Pr on the A sites, for instance in $PrSc_{1-x}Mg_xO_3$ [59] or even in $PrAlO_3$, depending on the annealing conditions [60]. What is striking in the $(Pr_{1-y}Sm_y)_{0.7}Ca_3CoO_3$ series is that the mixed valence only takes place below a certain transition temperature. To the best of our knowledge, there is only one previous case of that type, occurring in the double perovskite $Ba_2PrRu_{1-x}Ir_xO_6$ (for $0.1 \leq x \leq 0.4$), where it is related to the interplay between Ru^{5+} and Ir^{4+} [61,62].

In $(Pr_{1-y}RE_y)_{1-x}Ca_xCoO_3$, Naito *et al.* carried out a comprehensive study over broad ranges of *x*, *y* and various RE, to identify the structural parameters allowing to observe VSST [9]. It was concluded that it requires small enough r_A and some minimum degree of disorder in size, quantified by the atomic randomness $\sigma^2 = \sum_i z_i r_i^2 - \langle r_A \rangle^2$, where z_i and r_i are the concentration and ionic radius of each element in the A site, respectively [9]. Since VSST is intimately connected to the mixed valence of Pr, these criteria might be regarded as those necessary to induce a fraction of Pr^{4+} at low *T*. Note, however, that this approach could not account for the VSST in the archetypical compound $Pr_{0.5}Ca_{0.5}CoO_3$ for which σ^2 is very small.

Actually, the latest studies on cobaltates have suggested that the underlying parameter controlling the appearance of Pr^{4+} is rather the bond angle Co-O-Co. The apparent link between the VSST and the couple (r_A , σ^2) can be ascribed to the fact that Pr/RE substitution is in practice the easiest way to reduce this angle. It was also shown that the distortion of the CoO_6 octahedra plays also a role in itself, in such a way that an average value of Co-O-Co is only relevant in first approximation [63]. Comparing the structural parameters of $Pr_{0.5}Ca_{0.5}CoO_3$ (VSST), $Pr_{0.55}Ca_{0.45}CoO_3$ (no VSST) , and $Pr_{0.50}Y_{0.05}Ca_{0.45}CoO_3$ (VSST), García-Muñoz *et al.* claimed a leading role of the apical tilting of the CoO_6 octahedra [3], suggesting that the corresponding θ_1 angle should be below ~158 ° to allow the stabilization of a Pr^{4+} fraction at low *T*. Later, it was confirmed that such a critical angle can be consistent with the appearance of VSST for $x > 0.45$ within the fully oxygenated $Pr_{1-x}Ca_xCoO_3$ series [45]. In the present study on $(Pr_{1-y}Sm_y)_{0.7}Ca_{0.3}CoO_3$, however, Fig. 1(b) shows that the θ_1

corresponding to y_{crit} ~ 0.18 is noticeably lower, being close to 157.2°. At this stage, it is difficult to know whether this discrepancy is just a matter of experimental uncertainties, or if it rathers indicates that the complexity of the charge transfer in these cobaltates cannot be reduced to a single angle, independently of other important parameters such as the doping level.

C. Chemical composition and VSST

Experimentally, the VSST has been observed only in perovskites of formula $ACoO_3$, with Pr and Ca on the A sites. We have seen that the basic ingredients to get a VSST are the existence —at low *T*— of a RE in a mixed valence and of Co^{3+} in the LS state. Strikingly, it turns out that this RE can only be Pr in practice [13,64]; none of the other RE susceptible to exhibit a mixed valence (e.g. Tb) can in itself trigger the VSST [12]; it is probably a matter of hybridization with the O *2p* orbitals and respective positioning of the RE and Co bands [13]. On the basis of electronic-structure calculations, Knížek *et al.* evidenced the existence of a broad Pr $4f^2$ band located just below the Fermi level of $Pr_{0.5}Ca_{0.5}CoO_3$; replacing Pr by its closest neighbor Nd makes this feature disappear [13].

Therefore, the set of conditions to get VSST can be rewritten as : (i) presence of Pr at the A sites, (ii) mixed valence Co^{3+}/Co^{4+} to accommodate the change in Pr valence, and (iii) average A site radius below a limit value, in order to get Co-O-Co small enough to stabilize at low *T* the Co^{3+} in LS state and a fraction of Pr^{4+}. In practice (ii) requires the incorporation of a divalent alkaline earth, and (iii) requires that it is Ca^{2+}, since obeying this "size condition" is impossible with other usual divalent cations, like Sr^{2+} or Ba^{2+}. Finally, the combination of these various requirements to get VSST shows it is natural that this peculiar transition was observed only in $(Pr,Ca)CoO_3$ perovskites.

V. CONCLUSION

Investigation of several physical properties led us to build a phase diagram of the system $(Pr_{1-y}Sm_y)_{0.7}Ca_{0.3}CoO_3$ ($0 < y < 0.5$), tracking the variations of the VSST temperature *T**, the Curie temperature T_C, and the ferromagnetic short-range ordering (T_{SRO}). This diagram exhibits a competition between a FM regime (low *y*) and a VSST regime (high *y*), with a crossover between them taking place around y_{crit} ~ 0.18.

The first basic question is the origin of y_{crit}, an issue for which x-ray absorption spectroscopy quantifying the variation of Pr^{4+} versus *y* was decisive. The ratio Pr^{4+}/Pr is shown to increase from 0 ($y = 0$) till ~ 0.3 ($y = 0.5$), with an acceleration around y_{crit}. It is along this jump that the Pr^{4+}/Pr^{3+} ratio reaches a value large enough to make the Co^{4+}/Co^{3+} being shifted below the threshold for which $T_C < T^*$.

The second basic question is the underlying cause of such a stabilization of Pr^{4+}. We found that this phenomenon in $(Pr_{1-y}Sm_y)_{0.7}Ca_{0.3}CoO_3$ corresponds to an apical Co-O-Co being lower than ~157.2°, i.e. a value significantly smaller than the one reported in compounds closer to half-doping [3]. Despite this discrepancy that remains to be investigated, there is no doubt that the angles Co-O-Co play a very central role in the VSST systems since they also control the variations of $T_C(y)$ and $T^*(y)$.

In addition to the competition between FM and VSST transitions, we observed ferromagnetic short-range ordering over the whole *y* range, indicating the presence of diluted FM clusters. Their amount remains small, even in the FM-like regime, and it becomes very tiny above y_{crit}. Both the $T_C(y)$ and $T_{SRO}(y)$ lines were found to be consistent with a standard double-exchange mechanism. Our analysis led us to suggest that these FM signatures are

associated with clusters involving Co^{4+} LS/Co^{3+} HS embedded in a background involving Co^{4+} LS/Co^{3+} LS.

Finally, it must be stressed that several features of the VSST remain puzzling. For instance, our data confirmed previous studies on the point that there is a *y* value for which the first-order character of the VSST seems to be enhanced [65]. The cause of such an optimum [y ~ 0.3 for $(Pr_{1-y}Sm_y)_{0.7}Ca_{0.3}CoO_3$] is not obvious. Is the Pr^{4+} fraction too small for smaller *y* ? Is the cooperativity between the Pr and Co sublattices decreased for too large *y* ? These questions illustrate the fact that there is still much work to do before fully understanding the Valence and Spin State Transition in cobaltates.

ACKNOWLEDGMENTS

The authors acknowledge the European Synchrotron Radiation Facility for provision of synchrotron radiation facilities. We also thank the UK Science and Technology Facilities Council (STFC) for provision of ISIS Xpress Access neutron beamtime.

---

[1] S. Tsubouchi, T. Kyomen, M. Itoh, P. Ganguly, M. Oguni, Y. Shimojo, Y. Morii, and Y. Ishii, Phys. Rev. B **66**, 052418 (2002).
[2] A. J. Barón-González, C. Frontera, J. L. García-Muñoz, J. Blasco, and C. Ritter, Phys. Rev. B **81**, 054427 (2010).
[3] J. L. García-Muñoz, C. Frontera, A. J. Barón-González, S. Valencia, J. Blasco, R. Feyerherm, E. Dudzik, R. Abrudan, and F. Radu, Phys. Rev. B **84**, 045104 (2011).
[4] J. Herrero-Martín, J. L. García-Muñoz, S. Valencia, C. Frontera, J. Blasco, A. J. Barón-González, G. Subías, R. Abrudan, F. Radu, E. Dudzik, and R. Feyerherm, Phys. Rev. B **84**, 115131 (2011).
[5] J. Herrero-Martín, J. L. García-Muñoz, K. Kvashnina, E. Gallo, G. Subias, J. A. Alonso, and A. J. Barón-González, Phys. Rev. B **86**, 125106 (2012).
[6] J. Hejtmánek, Z. Jirák, O. Kaman, K. Knížek, E. Šantavá, K. Nitta, T. Naito, and H. Fujishiro, Eur. Phys. J. B. **86**, 305 (2013).
[7] T. Fujita, T. Miyashita, Y. Yasui, Y. Kobayashi, M. Sato, E. Nishibori, M. Sakata, Y. Shimojo, N. Igawa, Y. Ishii, K. Kakurai, T. Adachi, Y. Ohishi, and M. Takata, J. Phys. Soc. Jpn **73**, 1987 (2004).
[8] T. Fujita, S. Kawabata, M. Sato, N. Kurita, M. Hedo, and Y. Uwatoko, J. Phys. Soc. Jpn **74**, 2294 (2005).
[9] T. Naito, H. Sasaki, and H. Fujishiro, J. Phys. Soc. Jpn **79**, 034710 (2010).
[10] J. Hejtmánek, E. Šantavá, K. Knížek, M. Maryško, Z. Jirák, T. Naito, H. Sasaki, H. Fujishiro, Phys. Rev. B **82**, 165107 (2010).
[11] A. V. Kalinov, O. Yu. Gorbenko, A. N. Taldenkov, J. Rohrkamp, O. Heyer, S. Jodlauk, N. A. Babushkina, L. M. Fisher, A. R. Kaul, A. A. Kamenev, T. G. Kuzmova, D. I. Khomskii, K. I. Kugel, and T. Lorenz, Phys. Rev. B **81**, 134427 (2010).
[12] H. Fujishiro, T. Naito, D. Takeda, N. Yoshida, T. Watanabe, K. Nitta, J. Hejtmánek, K. Knížek, and Z. Jirák, Phys. Rev. B **87**, 155153 (2013).
[13] K. Knížek, J. Hejtmánek, P. Novák, and Z. Jirák, Phys. Rev. B **81**, 155113 (2010).
[14] H. Fujishiro, T. Naito, S. Ogawa, N. Yoshida, K. Nitta, J. Hejtmánek, K. Knížek, and Z. Jirák, J. Phys. Soc. Jpn **81**, 064709 (2012).
[15] F. Guillou, Q. Zhang, Z. Hu, C. Y. Kuo, Y.Y. Chin, H.J. Lin, C. T. Chen, A. Tanaka, L.H. Tjeng, and V. Hardy, Phys. Rev. B **87**, 115114 (2013).
[16] V. Hardy, F. Guillou, and Y. Bréard, J. Phys.: Condens. Matter **25**, 246003 (2013).

[17] J. M. Chen, J. M. Lee, S. C. Haw, S. A. Chen, V. Hardy, F. Guillou, S. W. Chen, C. Y. Kuo, C. W. Pao, J. F. Lee, N. Hiraoka, H. Ishii, K. D. Tsuei, and Z. Hu, Phys. Rev. B **90**, 035107 (2014).
[18] F. Guillou, K. Kummer, Y. Bréard, L. Hervé, and V. Hardy, Phys. Rev. B **95**, 174445 (2017).
[19] R.I. Smith, S. Hull, M.G. Tucker, H.Y. Playford, D.J. McPhail, S.P. Waller and S.T. Norberg, Rev. Sci. Instrum. **90**, 115101 (2019).
[20] O. Arnold, J.C. Bilheux, J.M. Borreguero, A. Buts, S.I. Campbell, L. Chapon, M. Doucet, N. Draper, R.Ferraz Leal, M.A. Gigg, V.E. Lynch, A. Markvardsen, D.J. Mikkelson, R.L. Mikkelson, R. Miller, K. Palmen, P. Parker, G. Passos, T.G. Perring, P.F. Peterson, S. Ren, M.A. Reuter, A.T. Savici, J.W. Taylor, R.J. Taylor, R. Tolchenov, W. Zhou, J. Zikovsky, Nucl. Instrum. Methods Phys. Res. A **764**, 156 (2014).
[21] J. Rodriguez-Carvajal, Physica B **192**, 55 (1993).
[22] A. Rogalev and F.Wilhelm, Phys. Met. Metall. **116**, 1285 (2015).
[23] See Supplemental Material at xxx for details about the signature of T_C on the *C(T)* curves, the shape of the *M(B)* curves at low *T*, the temperature dependence of the *MR*, the training and hysteretical effects at the VSST, the resistivity in the phase diagram, the criteria used to derive T_C, T^* and T_{SRO}, the Co spin state at room temperature from XAS, the magnetic investigation of the system $Pr_{1-x}Ca_xCoO_3$, the absence of signature of SRO around room temperature in $Pr_{0.7}Ca_{0.3}CoO_3$, the T_C versus $\langle r_A \rangle$ in $RE_{0.7}AE_{0.3}CoO_3$ perovskites, the Curie-Weiss response of Co in $Pr_{0.7}Ca_{0.3}CoO_3$, the Co magnetism from XMCD, the *MR* in $Pr_{0.7}Ca_{0.3}CoO_3$, and the structural parameters of $(Pr_{1-y}Sm_y)_{0.7}Ca_{0.3}CoO_3$ derived from tofPND.
[24] K. Kummer, A. Fondacaro, E. Jimenez, E. Velez-Fort, A. Amorese, M. Aspbury, F. Yakhou-Harris, P. van der Linden, and N. B. Brookes, J. Synchrotron Radiat. **23**, 464 (2016).
[25] G. Y. Wang, X. H. Chen, T. Wu, G. Wu, X. G. Luo, and C. H. Wang, Phys. Rev. B **74**, 165113 (2006).
[26] We present here the data for our highest field of 5 T in order to enhance the signal-to-noise ratio in the low susceptibility regime when approaching 400 K.
[27] K. Knížek, J. Hejtmánek, M. Maryško, P. Novák, E. Šantavá, Z. Jirák, T. Naito, H. Fujishiro, C. de la Cruz, Phys. Rev. B **88**, 224412 (2013).
[28] Z. Jirák, J. Hejtmánek, K. Knížek, M. Maryško, P. Novák, E. Šantavá, T. Naito, and H. Fujishiro, J. Phys.: Condens. Matter **25**, 216006 (2013).
[29] J. B. Goodenough, J. Phys. Chem. Solids **6**, 287 (1958).
[30] D. Phelan, K. P. Bhatti, M. Taylor, S. Wang, and C. Leighton, Phys. Rev. B **89**, 184427 (2014).
[31] M. Maryško, Z. Jirák , K. Knížek, P. Novák, J. Hejtmánek, T. Naito, H. Sasaki, and H. Fujishiro, J. Appl. Phys. **109**, 07E127 (2011).
[32] T. Naito, H. Fujishiro, T. Nishizaki, N. Kobayashi, J. Hejtmánek, K. Knížek, Z. Jirák, J. Appl. Phys. **115**, 233914 (2014).
[33] J.-Q. Yan, J.-S. Zhou, and J. B. Goodenough, Phys. Rev. B **69**, 134409 (2004).
[34] Y. Kobayashi, T. Mogi, and K. Asai, J. Phys. Soc. Jpn **75**, 104703 (2006).
[35] S. Tsubouchi, T. Kyomen, M. Itoh, and M. Oguni, Phys. Rev. B **69**, 144406 (2004).
[36] S. El-Khatib, S. Bose, C. He, J. Kuplic, M. Laver, J. A. Borchers, Q. Huang, J. W. Lynn, J. F. Mitchell, and C. Leighton, Phys. Rev. B **82**, 100411(R) (2010).
[37] G. Y. Wang, T. Wu, X. G. Luo,W. Wang, and X. H. Chen, Phys. Rev. B **73**, 052404 (2006). [38] A. Ikeda, S. Lee, T. T. Terashima, Y. H. Matsuda, M. Tokunaga, and T. Naito, Phys. Rev. B **94**, 115129 (2016).
[39] T. Moyoshi, K. Kamazawa, M. Matsuda, and M. Sato, Phys. Rev. B **98**, 205105 (2018).
[40] D. Phelan, M. J. Krogstad, N. J. Schreiber, R. Osborn, A. H. Said, H. Zheng, and S. Rosenkranz, Phys. Rev. B **100**, 054101 (2019).

[41] In a ninefold coordination, the ionic radii of Pr^{3+} and of Y^{3+} are 1.179 and 1.075 Å, respectively (while that if Sm^{3+} is 1.132 Å).
[42] A. K. Kundu, E. V. Sampathkumaran, K. V. Gopalakrishnan, and C. N. R. Rao, J. Magn. Magn. Mater. **281**, 261 (2004).
[43] S. Tsubouchi, T. Kyomen, M. Itoh, and M. Oguni, Phys. Rev. B **69**, 144406 (2004).
[44] A. K. Kundu, P. Nordblad, and C. N. R. Rao, J. Solid State Chem. **179**, 923 (2006).
[45] D. Phelan, Y. Suzuki, S. Wang, A. Huq, and C. Leighton, Phys. Rev. B **88**, 075119 (2013).
[46] I. Fita, R. Szymczak, R. Puzniak, I. O. Troyanchuk, J. Fink-Finowicki, Ya. M. Mukovskii, V. N. Varyukhin, and H. Szymczak, Phys. Rev. B **71**, 214404 (2005).
[47] C. Leighton, D. D. Stauffer, Q. Huang, Y. Ren, S. El-Khatib, M. A. Torija, J. Wu, J. W. Lynn, L. Wang, N. A. Frey, H. Srikanth, J. E. Davies, K. Liu, and J. F. Mitchell, Phys. Rev. B **79**, 214420 (2009).
[48] J.-S. Zhou, J.-Q. Yan, and J. B. Goodenough, Phys. Rev. B **71**, 220103 (2005).
[49] M. Tachibana, T. Yoshida, H. Kawaji, T. Atake, and E. Takayama-Muromachi, Phys. Rev. B **77**, 094402 (2008).
[50] N. B. Ivanova, N. V. Kazak, C. R. Michel, A. D. Balaev, and S. G. Ovchinnikov, Phys. Solid State **49**, 2126 (2007).
[51] Z. Jirák, J. Hejtmánek, K. Knížek and M. Veverka, Phys. Rev. B **78**, 014432 (2008).
[52] J. C. Burley, J. F. Mitchell, and S. Short, Phys. Rev. B **69**, 054401 (2004).
[53] M. A. Señaris-Rodríguez and J. B. Goodenough, J. Solid State Chem. **116**, 224 (1995).
[54] K. Knížek, Z. Jirák, J. Hejtmánek, and P. Novák, J. Phys.:Condens. Matter **18**, 3285 (2006).
[55] M. J. Hoch, S. Nellutla, J. van Tol, E. S. Choi, J. Lu, H. Zheng, and J. F. Mitchell, Phys. Rev. B **79**, 214421 (2009).
[56] S. M. Zhou, Y. Li, Y. Q. Guo, J. Y. Zhao, and L. Shi, Appl. Phys. Lett. **105**, 232408 (2014).
[57] This is further supported by the variation of *MR(B)* as a function of temperature (see [23]).
[58] K. Knížek, Z. Jirák, J. Hejtmánek, P. Henry, and G. André, J. Appl. Phys. **103**, 07B703 (2008).
[59] K. Sekizawa, M. Kitagawa, and Y. Takano, J. Magn. Magn. Mater. **177-181**, 541 (1998).
[60] M. Wencka, S. Vrtnik, M. Jagodič, Z. Jagličić, S. Turczynski, D. A. Pawlak, and J. Dolinšek, Phys. Rev. B **80**, 224410 (2009).
[61] M. Wakeshima, Y. Izumiyama, Y. Doi, and Y. Hinatsu, Solid State Commun. **120**, 273 (2001).
[62] J. Sannigrahi, D. T. Adroja, C. Ritter, W. Kockelmann, A. D. Hillier, K. S. Knight, A. T. Boothroyd, M. Wakeshima, Y. Hinatsu, J. F. W. Mosselmans, and S. Ramos, Phys. Rev. B **99**, 184440 (2019).
[63] P. Tong, Y. Wu, B. Kim, D. Kwon, J. M. S. Park, and B. G. Kim, Phys. Soc. Jpn **78**, 034702 (2009).
[64] Y. Kobayashi, Y. Terakado, and K. Asai, and H. Yasuoka, J. Phys. Soc. Jpn **83**, 104704 (2014).
[65] V. Hardy, Y. Bréard, and F. Guillou, J. Phys.:Condens. Matter **33**, 095801 (2021).
[66] M. Medarde, C. Dallera, M. Grioni, J. Voigt, A. Podlesnyak, E. Pomjakushina, K. Conder, Th. Neisius, O. Tjernberg, and S. N. Barilo, Phys. Rev. B **73**, 054424 (2006).
[67] K. Knížek, Z. Jirák, J. Hejtmánek, M. Veverka, M. Maryško, G. Maris, and T. T. M. Palstra, Eur. Phys. J. B. **47**, 213 (2005).